

# Numerical modelling of the Sydney Basin using temperature dependent thermal conductivity measurements

**Alexandre Lemenager\***  
Macquarie University  
alexandre.lemenager@students.mq.edu.au

**Craig O'Neill**  
Macquarie University  
craig.oneill@mq.edu.au

**Siqi Zhang**  
Macquarie University  
siqi.zang@mq.edu.au

*\*presenting author asterisked*

## SUMMARY

The Thermal structure of continental crust is a critical factor for geothermal exploration, hydrocarbon maturation and crustal strength, and yet our understanding of it is limited by our incomplete knowledge of its geological structure and thermal properties. One of the most critical parameters in modelling upper crustal temperature is thermal conductivity, which itself exhibits strong temperature dependence. In this study, finite-element geothermal models of the Sydney Basin are generated through the use of deal.II finite element libraries. Basin geometry and structure is adapted from Danis, et al. (2011), which quantified the extent of Triassic sediment, Permian coal measure, Carboniferous volcanics and Basement thickness. We find that temperature-dependent thermal conductivity result in lower lateral variation in temperature compared to constant thermal conductivity models. However, the average temperatures at depth are significantly higher when temperature-dependent thermal conductivity effects are included. A number of regions within the Sydney Basin demonstrate temperature above 150C at depths of less than 2000m in these models, for instance NW of Singleton exhibits a strong thermal anomaly, demonstrating the potential for geothermal prospectivity of the region from experimentally-constrained thermal parameters. Future work will address the repeatability and application of this type of thermal model in areas of varying geology and stratigraphy, as well as refining the model by adding new variables, such as pressure or fine tuning existing variables.

**Key words:** Sydney Basin; thermal conductivity; temperature dependent; thermal model

## INTRODUCTION

In this study, temperature dependent thermal conductivity measurements are implemented in thermal models to constrain the temperature distribution in the Sydney Basin at depth. Variables used to set-up the model have been adapted from Danis et al. (2012), who has produced thermal models of the Sydney Basin, based on constant thermal conductivity values. These thermal models were constrained using equilibrated borehole temperature measurements from shallow groundwater in the Sydney Basin. However, large scale effects of temperature dependent thermal conductivity have yet to be implemented in current models regarding the Sydney Basin.

This study aims to assess how much of an effect variable thermal conductivity has on the large scale temperature distribution of the Sydney Basin, particularly when compared against constant thermal conductivity models. To do this, finite element simulations were performed which result in a model of the temperature distributions of the Sydney Basin at depth, incorporating the effects of the basin stratigraphy, heat producing values and variations in thermal conductivity.

The thermal conductivity of Sydney Basin sediments (incorporating sandstone and coal) and basement (consisting of Lachlan Fold Belt granitoids) have a significant temperature dependence based on the measurements used in this study. It is currently thought that the addition of temperature dependent thermal conductivity data in geothermal simulations will result in significantly different temperature distributions at depth. For example, a drop in the thermal conductivity of sediments with increasing temperature, could result in greater simulated temperatures at depth, this constitutes critical information on the distribution of potential high temperature domains that may be prospective for geothermal energy.

## METHOD AND RESULTS

The ultimate aim of this project is to understand how temperature-dependent thermal conductivities, derived from new laboratory measurements, impact models of the thermal structure of the Sydney Basin. As such this work has two main prongs: i) to introduce new temperature-dependent conductivity measurements for the Sydney Basin, compile existing measurements, and collate related data, and ii) develop 2D deal.II finite element models for the thermal state of the Sydney Basin.

A number of datasets have had to be compiled in order to realistically characterise the model. The parameters which have been used to constrain the model include:

- Temperature dependent thermal conductivity of the geology and internal precision / standard deviation of thermal conductivity measurements
- Spatial information (large scale geology and elevation at a fine enough resolution)
- Equilibrated temperature extrapolations (extracted from borehole measurements at various depth)
- Heat production values (radiogenic heating)

## Thermal conductivity

A number of thermal conductivity precision test were undertaken on calibrating specimens to assess the instrument's precision. Each calibration specimen which consisted of a stainless steel 19.05mm thick cylinder, 3.175mm and 9.525mm vespel cylinders were tested three times excluding the initial calibration process. These measurements were compared to initial calibration values and their deviation from original measurements was recorded. Internal precision measurements were only done for low temperature set points. The uncertainty in thermal conductivity is highest at low temperature due to the fact that instrument equilibration is affected by ambient temperature at a greater extent, interfering with low temperature thermal conductivity tests. An average of the standard deviation at each temperature interval (20, 50, 100C) of the calibration specimens was calculated. A percentage of the standard deviation was then used to apply onto field samples in order to get a bearing on a realistic margin of error for each sample at specific temperatures.

## Finite element modelling

### Governing equations

While the target area is a stable basin, the present sedimentation rate is low (approximately ~65m/Ma, determined by Gulson et al. (1990)), and the temporal evolution and convection effect due to sedimentation is ignored in this study. As a result, we solve a stable heat conduction problem as the following form:

$$\nabla \cdot [k(T)\nabla T] + H = 0 \quad (1)$$

### Newton's Method

As thermal conductivity is temperature dependent, a non-linear scheme has to be implemented to solve this problem. Although convergence may be achievable using direct iteration, this is the case only while thermal conductivity is weakly dependent on temperature. In this study, as the partial derivative of thermal conductivity as a function of temperature is simple to approximate, we use a more complicated but faster converging Newton scheme.

The initial thermal field for the Newton iteration is found by solving Eq. 1 using thermal conductivity calculated from a constant temperature. Then, while the temperature  $T$  of the previous Newton step is known, the thermal conductivity expressed as  $K$  relative to the temperature used for the next step,  $T + \delta T$  can be approximated as:

$$k(T + \delta T) = k(T) + \frac{\partial k(T)}{\partial T} \delta T \quad (2)$$

The temperature change between steps  $\delta T$  are solved as ( $T$  is known from the previous Newton step):

$$\nabla \cdot \left( \frac{\partial k}{\partial T} \delta T \nabla T \right) + \nabla \cdot [k(T)\nabla \delta T] + \nabla \cdot [k(T) \cdot \nabla T] + H = 0 \quad (3)$$

This solving scheme normally give convergence within ~10 iterations for an error residual of 2.90655x10<sup>-6</sup> (for thermal profile 1).

### Deal.II libraries

To build our own code, an open source finite-element library – deal.ii (<https://www.dealii.org>) is used. It takes care of the details of most finite element codes, such as handling of grid, degrees of freedom, sparse matrices and provides support for different solvers, which helps keep our code manageable. Its dimensionally independent concept and excellent support for adaptive mesh refinement and massively parallel architectures gives great potential for easier future expansion of our code to more complicated 3D thermal models.

### Computation grid

When running simulations, the 2D computation domain is 60-180km in length, depending on profile location. Model depth is uniformly set to 12km, and the top surface is based on topography. The mesh is build based on a divided rectangular triangulation (divided to make each mesh cell close to a square), and further globally refined and transformed to fit the topography of the surface. So a global refinement value defines the model resolution. Through trial and error, a global refinement value of 6 (4,096 cells) to 7 (16,384 cells) was decided as it provided an effective compromise for simulation speed and resolution. Simulations with a global refinement value of 6 have a cell size of approximately 200mx200m, while simulations with a global refinement of 7 have a cell size of approximately 100mx100m, effectively quadrupling the resolution, however requiring more time to compute. In practice, an increased resolution rendered by a global refinement value of 7 doesn't seem to have noticeable changes on the results. Simulation time for a global refinement of 6 is very rapid may only take a few seconds, the same goes for a global refinement of 7, usually taking a minute to solve.

### Monte Carlo Method

Monte Carlo simulations were performed utilising a python script. An initial script was written to create directories with respect to the root configuration file, and data files (which contain  $H$  and  $K$  values, with standard deviations). A total of one thousand directories were generated, all of which have randomly selected thermal conductivity values, from a Gaussian distribution with measured means, and standard deviations. Once a simulation suite has completed, the output from all one thousand directories is compiled into singular plot files. Each plot file shows the mean, while adding and subtracting one standard deviation to show the uncertainty range. A geotherm is taken every 10km along each profile. Extracted geotherms provide a quantitative temperature range useful for determining the thermal arrangement of each profile. Increased iterations (10,000) per simulations are used to determine whether more iterations necessarily mean increased accuracy, as large simulations are computationally expensive and are a time consuming process.

**Physical model set up**

The full geological model is constructed as a series of 12 geological profiles, which define the geometry of the major lithological units for all modelled profiles. Heat production values, and variable conductivity are provided for each layer used in the individual models.

*Boundary conditions*

A surface temperature of 15°C is used, as indicated by Danis et al. (2012). This value is taken from Cull (1989) measurements. A bottom temperature of 350°C at 12km is used, which is the modelled temperature used by Danis et al. (2012) in their models. Side conditions of the model have no heat flow, meaning that boundary temperatures are all accounted for at the top and bottom of the model. Excluding heat flow from side conditions ensures that the model is internally consistent by minimizing edge effects.

*Interpolation method*

The Lagrange interpolation helps finding the exact value between known data points. Assuming a global refinement value of 6 is used for all simulations, the mesh would be defined by an approximately 200x200m cell size, while a global refinement of 7 would mean a cell size of approximately 100x100m, slight variations would depend on initial profile dimensions. In order to reliably predict fine resolution basin geometry with an adequate lateral resolution, an interpolation method was required. The Lagrange high order interpolating polynomial is used in this case to get a complete distribution between data points for multiple datasets. As a result, the 'void' between real data points is reduced by estimating intermediate data points through 3rd order Lagrange interpolation. A polynomial that passes through and interpolates n+1 coordinates is constructed for all following data points (x0, y0), (x1,y1)...(x3,y3). A sequential list of values (x0, x1, x2, x3) starting from the beginning of the profile are used to define interpolating polynomials, where for instance:

$$y = jx^3 + kx^2 + mx + c$$

In this case: j, k, m, and c are constants associated with initial values the polynomial was calculated from. This polynomial would intersect all points defined by the interpolating functions.

*Spatial information*

The basin geometry used to characterise the geothermal models generated in this study has been taken from the raw data component of the gravity modelling undertaken by Danis et al. (2011). The model is divided into a total of 12 profiles, which extend laterally W-E along the length of the Sydney Basin. As a result, all profiles vary in size. This method was opted for as it retains consistency with models constructed by Danis et al. (2011/2012) and serves as a useful platform for direct comparison. The traverse length of each profile was extracted from published figures in Danis et al. (2011/2012) by digitizing each respective longitude and latitude. Once the traverse length is established, the following equation is used to provide the distance in meters from the western most point of the Sydney Basin to the eastern most point, which would be determined by its coastal outline.

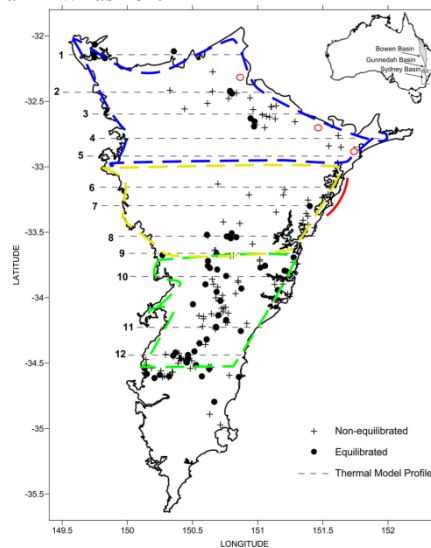
All profiles have known latitudes, which is transformed into 2D Cartesian form. We calculate the horizontal coordinate as:

$$x = R_e \cos\left(\frac{\text{lat}}{180} * \pi\right) * \frac{\text{lon1} - \text{lon0}}{180} * \pi$$

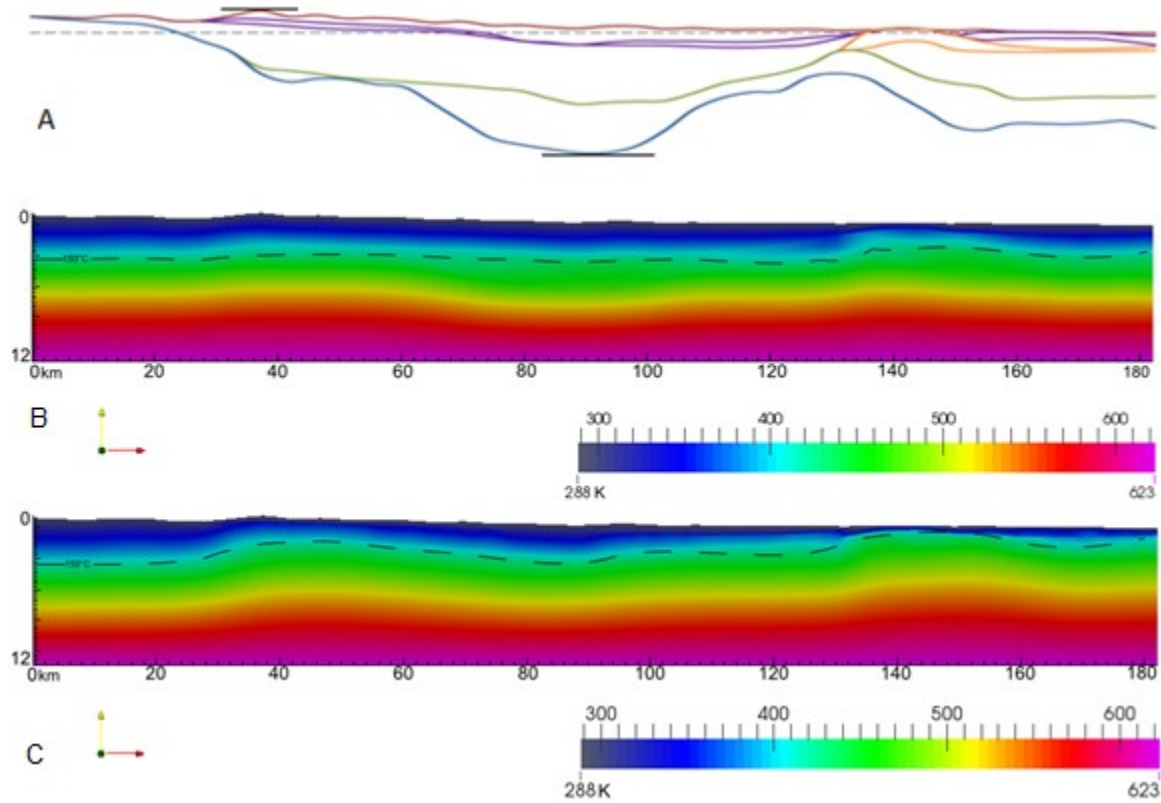
Re is the radius of the earth, lat is the latitude of the profile, lon0 and lon1 are the longitude of the target and starting points respectively.

*Profile geometry*

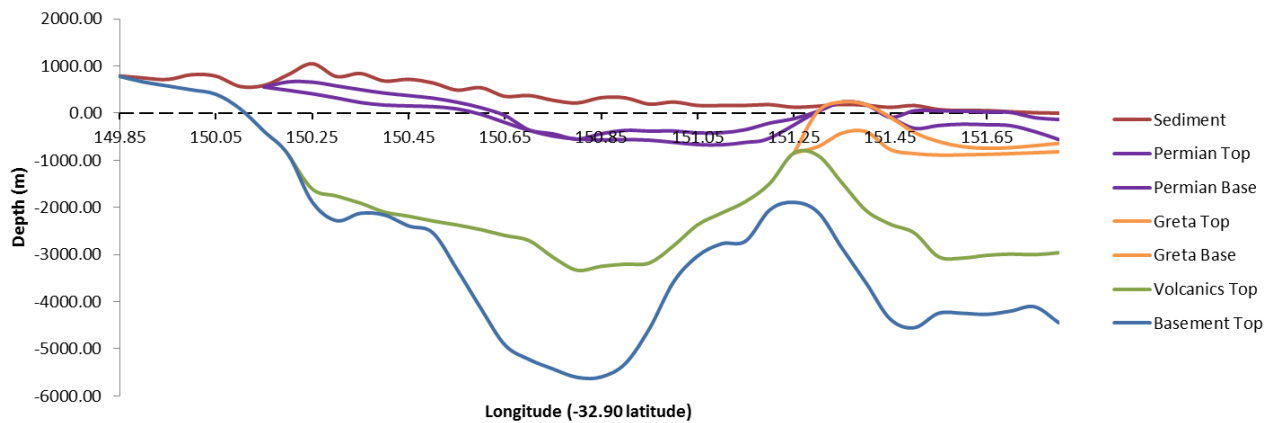
All profiles have been designed with 4 layers consisting of a Triassic sedimentary layer, a Permian coal layer, a Carboniferous volcanics layer and a Carboniferous Basement layer. Profiles 1-6 have the most complex geometry with one additional 'Greta' coal layer overlain by the Permian coal layer. The sedimentary layer is defined down to the basal volcanics layer, and a coal layer/s intermittently within this unit. Bottom of the basement is not depicted in following profiles; however simulations assume a basement limit of 12 km, profiles are all orientated in an E-W fashion.



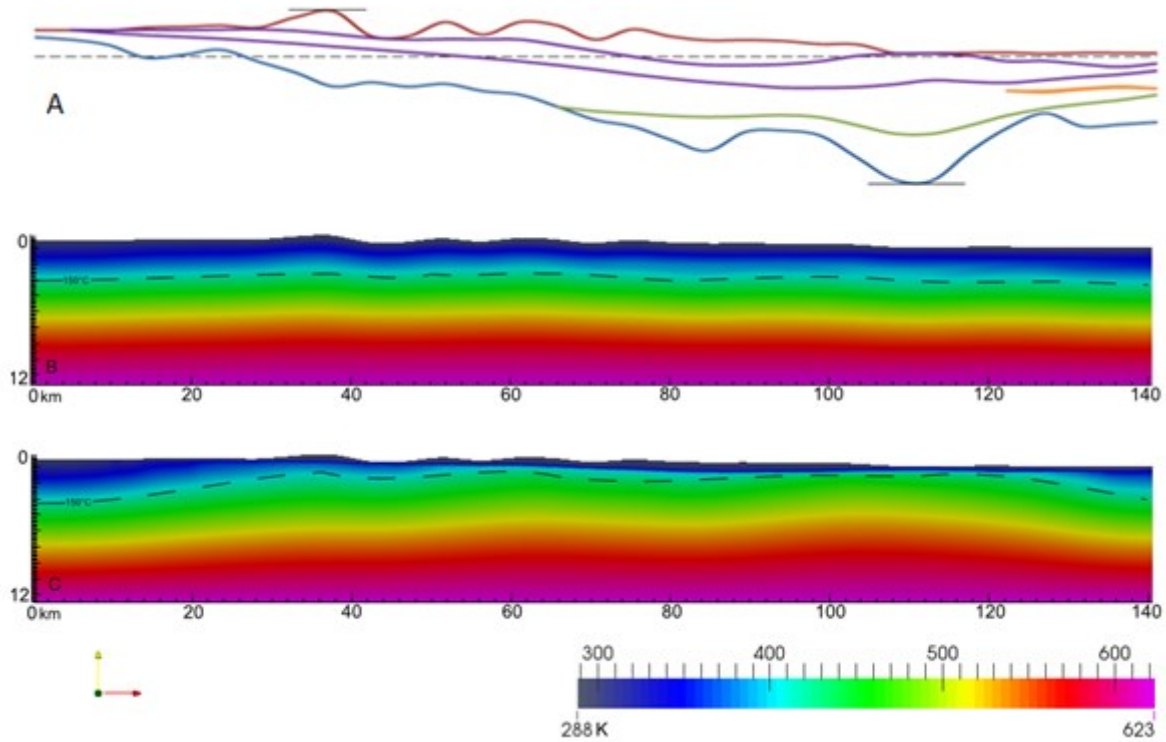
**Map 1: Plan view of the Sydney Basin with coordinates, showing location of profile lines 1 to 12, adapted from Danis et al. (2012). Blue, yellow and green lines show the outline of different basement types, including Gulgong, Bathurst and Wyangala respectively. Red circles show coal sampling locations, and the red line shows the sediments sampling locations.**



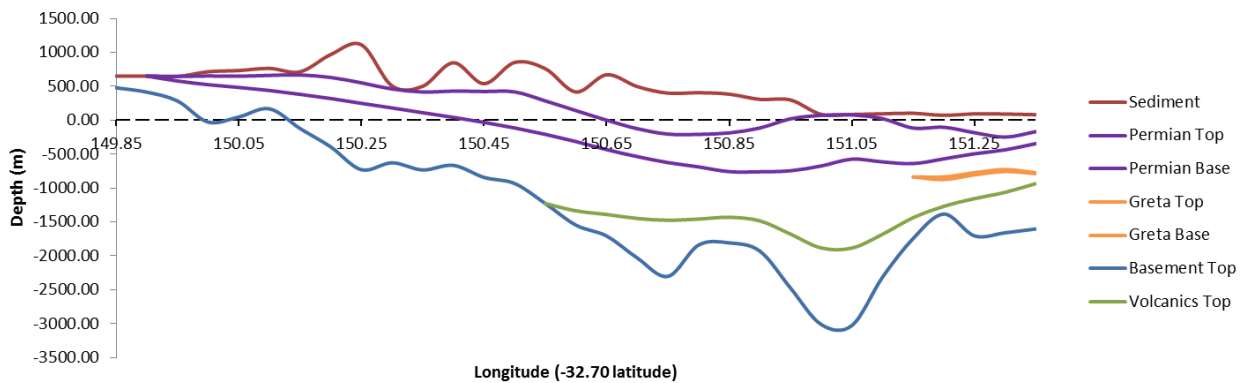
**Profile 5 extracts.** Red line represents sediments, purple lines represent the Permian coal measures, orange lines represent the Greta coal measures, the green line represents the Carboniferous volcanics, and the blue line represents the top of the basement. This collage shows the effect of the thick Greta coal measures on subsurface temperatures. A) Lithological model, as described in chapter 3, top topography is 1050m and deepest point for top of basement is 5605m B) Subsurface temperatures for temperature dependent thermal conductivity within each geological unit, from table 4.1. C) Subsurface temperature for constant thermal conductivity within each geological unit.



**Detailed figure of profile 5 with unit names and specific elevations in meters.**



**Profile 3 extracts. Red line represents sediments, purple lines represent the Permian coal measures, orange lines represent the Greta coal measures, the green line represents the Carboniferous volcanics, and the blue line represents the top of the basement. Effect of topography and thick Permian coal measures on subsurface temperatures. A) Lithological model, as described in chapter 3, top topography is 1113m and deepest point for top of basement is 3027m B) Subsurface temperatures for temperature dependent thermal conductivity within each geological unit, from table 4.1. C) Subsurface temperature for constant thermal conductivity within each geological unit.**



**Detailed figure of profile 3 with unit names and specific elevations in meters.**

### CONCLUSIONS

The initial aims of this study have been to compile and incorporate the basin geometry and temperature dependent thermal conductivity measurements and constant thermal conductivity values in thermal models of the Sydney Basin, and assess their relevance in terms of their effect on thermal structure.

It was found, that temperature dependent thermal models have much more restrained isotherms than non-temperature dependent thermal models. This is primarily thought to be due to the presence of coal measures, insulating heat generating basement, as well as the reduction in thermal conductivity of the sediments with temperature. Basement architecture and proximity to surface also impacts the results, where the lack of sediment in some cases leads to thermal refraction patterns. Geotherm plots were used to show the uncertainty range of thermal gradients in order to confidently estimate temperatures at depth. However, the main findings of this research consist of the highly temperature dependent nature of thermal models and the impact of thermal conductivity variation on the thermal structure of the Sydney Basin.

Geotherm plots indicate the apparent viability for geothermal potential in the Sydney Basin. 1D geotherm plots suggesting the appearance of 150°C isotherms at relatively shallow depths, which are ideal as exploration targets. The range of potential sites include the North West Singleton, Wollemi National Park, Central Blue Mountains, South Katoomba and Stanwell Park vicinity, showing potential at 2km or less. North West of Singleton is thought to be the most appropriate site for possible geothermal exploration, localised thermal models would help to further constrain geothermal potential.

New understanding of the Sydney Basin thermal structure could lead to new research targets regarding geothermal potential of the Sydney Basin. The Sydney Basin may be used as a proxy for the understanding of other sites that share similar geology. This could also perhaps prompt future interest in investing in geothermal energy both in Australia and elsewhere.

#### ACKNOWLEDGMENTS

I would like to sincerely thank my supervisors, Craig O'Neill and Siqi Zhang who have taught me a lot and guided me through the world of academic research. A lot is still to be learnt, but I very much their repeated guidance and help along the way. I thank my peers who are also submitting their theses for all the moral support they have provided in times of need. I thank my family and friends who showed interest in my project and offered assistance when nothing was asked of them. And last but not least I would like to thank my parents especially for keeping a roof under my head and always being there for me.

This thesis is dedicated to those people and I wish fortune to all of those who have partaken in this thrilling journey of academic research, through the Macquarie University Master of Research program. Lastly I would like to thank CCFS for research funding and for the incredible research this program has produced over the years since its inception.

#### REFERENCES

- Abdulagatova, Z., Abdulagatov, I. M., & Emirov, V. N. (2009). Effect of temperature and pressure on the thermal conductivity of sandstone. *International Journal of Rock Mechanics and Mining Sciences*, 46(6), 1055-1071.
- Alishaev, M. G., Abdulagatov, I. M., & Abdulagatova, Z. Z. (2012). Effective thermal conductivity of fluid-saturated rocks: experiment and modeling. *Engineering Geology*, 135, 24-39.
- Bangerth, W., Hartmann, R., Kanschä, G. (2007). Deal.II – a general purpose object orientated finite element library. *ACM Transactions on Mathematical Software (TOMS)*, 33(4), 1-24.
- Blevin, P.; Chappell, B.; and Jeon, H. (2010). Heat generating potential of igneous rocks within and underlying the Sydney Basin: some preliminary observations. *Proceedings of the 37th Symposium of the geology of the Sydney Basin*.
- Casareo, F. (1996). *Geochemical and petrographic studies of coals in the upper Permian Whittingham coal measures, Northern Sydney Basin, NSW, Australia*. North Ryde: Macquarie University.
- Clauser, C., & Huenges, E. (1995). Thermal conductivity of rocks and minerals. *Rock physics & phase relations: A handbook of physical constants*, 105-126.
- Conaghan, P. J., Jones, J. G., McDonnell, K. L., & Royce, K. (1982). A dynamic fluvial model for the Sydney Basin. *Journal of the Geological Society of Australia*, 29(1-2), 55-70.
- Conaghan, P., Jones, G., & McDonnell, K. (1987). Coal measures of an orogenic recess: Late Permian Sydney Basin, Australia. *Paleogeography, Paleoclimatology, Paleoecology*, 58(3-4), 203-219.
- Danis, C., & O'Neill, C. (2010). A static method for collecting temperatures in deep groundwater bores for geothermal exploration and other applications. *Proceedings of Groundwater*.
- Danis, C., O'Neill, C., Lackie, M., Twigg, L., Danis, A. (2011). Deep 3D structure of the Sydney Basin using gravity modelling, *Australian Journal of Earth Sciences: An International Geoscience Journal of the Geological Society of Australia*, 58(5), 517-542.
- Danis, C., O'Neill, C. Lee, J. (2012). Geothermal state of the Sydney Basin: assessment of constraints and techniques, *Australian Journal of Earth Sciences: An International Geoscience Journal of the Geological Society of Australia*, 59(1), 75-90.
- Danis, C. (2014). Use of groundwater temperature data in geothermal exploration: the example of Sydney Basin, Australia. *Hydrogeology Journal*, 22(1), 87-106.
- Evans, M. (2013). *Thermal conductivity database of Paleozoic intrusives of Basement to the Sydney Basin*. Department of Earth and Planetary Sciences, Macquarie University.
- Facer, R. A.; Cook, A. C.; and Beck, A. E. (1980). Thermal properties and coal rank in rocks and coal seams of the Southern Sydney Basin, NSW: a palaeogeothermal explanation of coalification. *International Journal of Coal Geology*, 1(1), 1-17.
- Finlayson, D. M. & H. M. McCracken, H. M. (1981) Crustal structure under the Sydney Basin and Lachlan Fold Belt, determined from explosion seismic studies, *Journal of the Geological Society of Australia: An International Geoscience Journal of the Geological Society of Australia*, 28(1-2), 177-190.
- Gerner EJ, Holgate FL (2010) OzTemp Interpreted temperature at 5 km depth image. Available via Geoscience Australia. <http://www.ga.gov.au/energy/geothermal-energy-resources.html>, Accessed 4 May 2011

- Goff, J. A., & Holliger, K. (Eds.). (2012). Heterogeneity in the crust and upper mantle: nature, scaling, and seismic properties. Springer Science & Business Media.
- Gulson, B. L., Diessel, C. F. K., Mason, D. R., & Krogh, T. E. (1990). High precision radiometric ages from the northern Sydney Basin and their implication for the Permian time interval and sedimentation rates. *Australian Journal of Earth Sciences*, 37(4), 459-469.
- Greenhalgh, S. A.; Suprajitno, M.; & King, D. W. (1986). Shallow seismic reflection investigation of coal in the Sydney Basin. *Geophysics*, 51(7), 1426-1437.
- Heller, P. L., Angevine, C. L., Winslow, N. S., & Paola, C. (1988). Two-phase stratigraphic model of foreland-basin sequences. *Geology*, 16(6), 501-504.
- Herbert, C. (1995) Sequence stratigraphy of the Late Permian Coal Measures in the Sydney Basin, *Australian Journal of Earth Sciences: An International Geoscience Journal of the Geological Society of Australia*, 42(4), 391-405.
- Hunt, J., Anderson, A., Benett, A., Brakel, A., & Whithouse, J. (1984). Petrography and geochemistry of the coals and depositional environments of the sediments in the late Permian Tomago and Newcastle coal measures from the bore Strevens Terrigal 1 - Northern Eastern Sydney Basin, NSW. North Ryde: CSIRO - Institute of Energy and Earth Resources.
- Jones, J. G., Conaghan, P. J., & McDonnell, K. L. (1987). Coal measures of an orogenic recess: late Permian Sydney Basin, Australia. *Palaeogeography, palaeoclimatology, palaeoecology*, 58(3), 203-219.
- Petrini, K., & Podladchikov, Y. (2000). Lithospheric pressure-depth relationship in compressive regions of thickened crust. *Journal of Metamorphic Geology*, 18(1), 67-78.
- Jaupart, C., & Mareschal, J. C. (2005). Production from Heat Flow Data. *The Crust*, 3, 65.
- Quenette, S., Moresi, L., O'Neill, C., & Danis, C. (2012). The effects of temperature dependent thermal conductivity on basin heat flow. Thirty-Seventh Workshop on Geothermal Reservoir Engineering.
- Qureshi, I. R. (1989) Positive gravity anomaly over the Sydney Basin. *Exploration Geophysics*, 20(1-2), 191-193.
- Rawling, T.J., Sandiford, M., Beardsmore, G.R., Quenette, S., Goyen, S.H. and Harrison, B.: Thermal insulation and geothermal targeting, with specific reference to coal-bearing basins, *Australian Journal of Earth Sciences*, 60, (2014), 817-829.
- Regenauer-Lieb, K., Weinberg, R. F., & Rosenbaum, G. (2006). The effect of energy feedbacks on continental strength. *Nature*, 442(7098), 67-70.
- Rezaei, H. R., Gupta, R. P., Bryant, G. W., Hart, J. T., Liu, G. S., Bailey, C. W., ... & Endo, Y. (2000). Thermal conductivity of coal ash and slags and models used. *Fuel*, 79(13), 1697-1710.
- Turcotte, D. L., & Schubert, G. (2014). *Geodynamics*. Cambridge University Press.
- Vila, M.; Fernandez, M.; Jimenez-Munt, I. (2010). Radiogenic heat production variability of some common lithological groups and its significance to lithospheric thermal modelling. *Technophysics*, 49(5), 152-164.
- Vosteen, H. D., & Schellschmidt, R. (2003). Influence of temperature on thermal conductivity, thermal capacity and thermal diffusivity for different types of rock. *Physics and Chemistry of the Earth, Parts A/B/C*, 28(9), 499-509.